Carbenes As Catalysts for Transformations of Organometallic Iron Complexes

Vincent Lavallo, *et al.*

Science **326**, 559 (2009);
DOI: 10.1126/science.1178919

The following resources related to this article are available online at www.sciencemag.org (this information is current as of October 29, 2009):

Updated information and services, including high-resolution figures, can be found in the online version of this article at:
http://www.sciencemag.org/cgi/content/full/326/5952/559

Supporting Online Material can be found at:
http://www.sciencemag.org/cgi/content/full/326/5952/559/DC1

A list of selected additional articles on the Science Web sites **related to this article** can be found at:
http://www.sciencemag.org/cgi/content/full/326/5952/559#related-content

This article **cites 33 articles**, 7 of which can be accessed for free:
http://www.sciencemag.org/cgi/content/full/326/5952/559#otherarticles

This article has been **cited by** 1 articles hosted by HighWire Press; see:
http://www.sciencemag.org/cgi/content/full/326/5952/559#otherarticles

This article appears in the following **subject collections**:
Chemistry
http://www.sciencemag.org/cgi/collection/chemistry

Information about obtaining **reprints** of this article or about obtaining **permission to reproduce this article** in whole or in part can be found at:
http://www.sciencemag.org/about/permissions.dtl

Downloaded from www.sciencemag.org on October 29, 2009

Science (print ISSN 0036-8075; online ISSN 1095-9203) is published weekly, except the last week in December, by the American Association for the Advancement of Science, 1200 New York Avenue NW, Washington, DC 20005. Copyright 2009 by the American Association for the Advancement of Science; all rights reserved. The title *Science* is a registered trademark of AAAS.

*a*NHCs are more basic than NHCs. Indeed, calculations predict that the first (287.0 kcal mol^{-1}) and second (144.6 kcal mol^{-1}) proton affinity of *a*NHC **9** are significantly higher than those of normal NHCs (229.9 to 270.6 and 38.9 to 106.5 kcal mol^{-1}, respectively) (*38*).

Although abnormal NHC **9** is sensitive to air and quantitatively rearranges to **8** upon heating in benzene at 50°C for 48 hours, it is stable at room temperature for a few days both in the solid state (melting point: decomposition at 65°C) and in solution (*39*). The availability of stable *a*NHCs not only provides easy access to a variety of transition-metal complexes, but also allows for their use as organocatalysts. As a proof of concept (*40*–*43*), (*a*NHC)AuCl complex **10** and (*a*NHC)-CO_2 adduct **11** have been prepared in 79 and 95% isolated yields by simply reacting **9** with chloro(dimethylsulfide)gold(I) and CO_2, respectively (Fig. 2).

Because the substituent at the C4 of **9** is a nonbulky benzene ring, a variety of substitution patterns should be tolerated without precluding isolation of the corresponding *a*NHC. The substituent at C4 is in conjugation with the carbene center, which opens the possibility of substantially modulating the electronic character of the ring system.

References and Notes

1. R. A. Moss, M. S. Platz, M. Jones Jr., Eds., *Reactive Intermediate Chemistry* (Wiley, New York, 2004).
2. A. Igau, H. Grützmacher, A. Baceiredo, G. Bertrand, *J. Am. Chem. Soc.* **110**, 6463 (1988).
3. D. Bourissou, O. Guerret, F. P. Gabbaï, G. Bertrand, *Chem. Rev.* **100**, 39 (2000).
4. A. J. Arduengo III, R. L. Harlow, M. Kline, *J. Am. Chem. Soc.* **113**, 3122 (1991).
5. A. J. Arduengo III, *Acc. Chem. Res.* **32**, 913 (1999).
6. F. E. Hahn, M. C. Jahnke, *Angew. Chem. Int. Ed.* **48**, 950 (2008).
7. S. Díez-González, N. Marion, S. P. Nolan, *Chem. Rev.* **109**, 3612 (2009).
8. J. C. Y. Lin *et al.*, *Chem. Rev.* **109**, 3561 (2009).
9. C. Samojłowicz, M. Bieniek, K. Grela, *Chem. Rev.* **109**, 3708 (2009).
10. R. H. Grubbs, *Angew. Chem. Int. Ed.* **45**, 3760 (2006).
11. S. E. Denmark, G. L. Beutner, *Angew. Chem. Int. Ed.* **47**, 1560 (2008).
12. N. Marion, S. Diez-Gonzalez, S. P. Nolan, *Angew. Chem. Int. Ed.* **46**, 2988 (2007).
13. D. Enders, O. Niemeier, A. Henseler, *Chem. Rev.* **107**, 5606 (2007).
14. N. E. Kamber *et al.*, *Chem. Rev.* **107**, 5813 (2007).
15. S. Gründemann, A. Kovacevic, M. Albrecht, J. W. Faller, R. H. Crabtree, *Chem. Commun.* (*Camb.*) **21**, 2274 (2001).
16. G. Sini, O. Eisenstein, R. H. Crabtree, *Inorg. Chem.* **41**, 602 (2002).
17. The classification of *a*NHCs as carbenes is debatable, because in contrast to NHCs (Fig. 1, **I/I′**), the fully delocalized structure **III′** prevails over the imidazol-5-ylidene resonance form **III** (*18*). These structures fit into the definition of mesoionic compounds (*19*, *20*) and could be named 5-dehydroimidazolium ylides.
18. R. Tonner, G. Heydenrych, G. Frenking, *Chem. Asian J.* **2**, 1555 (2007).
19. International Union of Pure and Applied Chemistry, *Compendium of Chemical Terminology*, A. D. McNaught, A. Wilkinson, Eds. (Blackwell Scientific, Oxford, ed. 2, 1997).
20. An XML online corrected version of (*19*) is available at http://goldbook.iupac.org (2006), created by M. Nic, J. Jirat, B. Kosata; updates compiled by A. Jenkins are available at http://goldbook.iupac.org/M03842.html.
21. O. Schuster, L. Yang, H. G. Raubenheimer, M. Albrecht, *Chem. Rev.* **109**, 3445 (2009).
22. M. Albrecht, *Chem. Commun.* (*Camb.*) **31**, 3601 (2008).
23. P. L. Arnold, S. Pearson, *Coord. Chem. Rev.* **251**, 596 (2007).
24. H. Lebel, M. K. Janes, A. B. Charette, S. P. Nolan, *J. Am. Chem. Soc.* **126**, 5046 (2004).
25. A. Prades, M. Viciano, M. Sanau, E. Peris, *Organometallics* **27**, 4254 (2008).
26. M. Heckenroth, E. Kluser, A. Neels, M. Albrecht, *Angew. Chem. Int. Ed.* **46**, 6293 (2007).
27. M. Alcarazo *et al.*, *J. Am. Chem. Soc.* **127**, 3290 (2005).
28. A. M. Magill, B. F. Yates, *Aust. J. Chem.* **57**, 1205 (2004).
29. A. M. Magill, K. J. Cavell, B. F. Yates, *J. Am. Chem. Soc.* **126**, 8717 (2004).
30. S. Bambirra, D. V. Leusen, A. Meetsma, B. Hessen, J. H. Teuben, *Chem. Commun.* (*Camb.*) **4**, 522 (2003).
31. M. I. Korotkikh, A. V. Kiselov, T. M. Pekhtereva, O. P. Shvaika, *Ukrainskii Khim. Z.* **67**, 97 (2001).
32. Preparation methods and spectroscopic data for compounds **6** through **11** and computational details are available as supporting material on *Science* Online.
33. L. N. Appelhans *et al.*, *J. Am. Chem. Soc.* **127**, 16299 (2005).
34. Because of the counterion ($HX{\bullet}X^-$, where X is Cl or Br), two equivalents of base are needed.
35. R. W. Alder *et al.*, *Angew. Chem. Int. Ed.* **43**, 5896 (2004).
36. V. Lavallo, Y. Ishida, B. Donnadieu, G. Bertrand, *Angew. Chem. Int. Ed.* **45**, 6652 (2006).
37. V. Lavallo, Y. Canac, B. Donnadieu, W. W. Schoeller, G. Bertrand, *Science* **312**, 722 (2006).
38. R. Tonner, G. Heydenrych, G. Frenking, *Chem. Phys. Chem.* **9**, 1474 (2008).
39. The addition of LiBr or [12]crown-4 to a benzene solution of *a*NHC **9** does not catalyze the rearrangement into **8**. In contrast, the addition of both LiBr and [12]crown-4 induces the transformation of **9** into **8** at room temperature, suggesting that the free bromide anion facilitates the proton transfer, through hydrogen bonding, in agreement with previous works (*33*).
40. Gold-catalyzed reactions (*41*) and NHC-CO_2 adducts (*42*, *43*) have recently attracted considerable interest.
41. B. H. Lipshutz, Y. Yamamoto, *Chem. Rev.* **108**, 2793 (2008).
42. L. Delaude, *Eur. J. Inorg. Chem.* 1681 (2009).
43. S. N. Riduan, Y. Zhang, J. Y. Ying, *Angew. Chem. Int. Ed.* **48**, 3322 (2009).
44. We thank NIH (grant R01 GM 68825) and the Deutsche Forschungsgemeinschaft for financial support of this work and the Consejo Nacional de Ciencia y Tecnología (E.A.P.) and Alexander von Humboldt Foundation (P.P.) for postdoctoral fellowships. Metrical data for the solid-state structures of **6** (Br^-), **8**, **9**, and **10** are available free of charge from the Cambridge Crystallographic Data Centre under reference numbers CCDC-735754, CCDC-735755, CCDC-735756, and CCDC-744123, respectively.

Supporting Online Material
www.sciencemag.org/cgi/content/full/326/5952/556/DC1
Materials and Methods
References

24 June 2009; accepted 14 September 2009
10.1126/science.1178206

Carbenes As Catalysts for Transformations of Organometallic Iron Complexes

Vincent Lavallo and Robert H. Grubbs*

Compared with the enormous arsenal of catalysts used to produce organic compounds, complementary species that are able to mediate sophisticated organometallic transformations are virtually nonexistent. We found that stable N-heterocyclic carbenes (NHCs) can mediate unusual organometallic transformations in solution at room temperature. Depending on the choice of NHC initiator, stoichiometric or catalytic reactions of bis(cyclooctatetraene)iron $[Fe(COT)_2]$ ensue. The stoichiometric reaction leads to the isolation of a previously unknown mixed-valent species, featuring distinct and directly bonded Fe(0) and Fe(I) centers. In the catalytic process, three iron atoms are fused to afford the tri-iron cluster $Fe_3(COT)_3$, which is a hydrocarbon analog of Dewar's classic $Fe_3(CO)_{12}$ complex. The key step in both of these processes is proposed to involve the NHC's ability to induce metal–metal bond formation. These NHC-mediated reactions provide a foundation on which to develop future organometallic transformations that are catalyzed by organic species.

Carbenes are compounds with a neutral divalent carbon atom that feature either two singly occupied nonbonding orbitals (a triplet state) or a lone pair and an accessible vacant orbital (a singlet state). With only six electrons in its valence shell, the carbene center defies the octet rule, and for many years, carbenes were considered to be prototypical reactive intermediates (*1*). The view that carbenes could exist only as transient species was shattered in the late 1980s and early 1990s by the isolation of singlet phosphinosilyl (*2*) and N-heterocyclic carbenes (NHCs) (*3*), respectively, that were able to be bottled. These pioneering studies paved the way for the current revolution in carbene chemistry, which has rapidly developed over the past two decades (*4*–*7*). Although fundamental interest has contributed, the primary driving force for the explosion of research in this area is that NHCs and related species (*8*, *9*) have great synthetic utility.

Acting as strong electron donors, such species readily bind other molecules (*10*–*13*). Two of the best-known exploitations of this property are the

---

Arnold and Mabel Beckman Laboratory of Chemical Synthesis, Division of Chemistry and Chemical Engineering, California Institute of Technology, Pasadena, CA 91125, USA.

*To whom correspondence should be addressed. E-mail: rhg@caltech.edu

use of NHCs as ancillary ligands for transition-metal catalysts (*4*–*7*) and as organocatalysts in their own right (*14*). The former application often renders transition-metal species far more active and selective than classical phosphine-based systems, as exemplified by the current NHC-supported ruthenium olefin metathesis catalysts (*15*, *16*). The latter application, so-called organocatalytic carbene catalysis, is rooted in the pioneering studies of Breslow (*17*), which implicated transient NHCs as intermediates in the thiamine-promoted benzoin condensation reaction. The use of stable NHCs, particularly Enders' triazolylidenes (*18*), in place of thiamine has led to highly efficient systems for the benzoin condensation and related reactions, as well as numerous distinct transformations (*14*, *19*, *20*). The unifying theme in these metal- and carbene-catalyzed approaches is that they both mediate organic transformations to produce organic molecules of potential interest, ranging from materials to pharmaceuticals.

What if it were possible to use NHCs in a different manner; namely, to catalyze organometallic transformations, resulting in metal–metal (M–M) bond formation? Organometallic compounds containing direct M–M bonds often display fascinating structures and play a key role in our understanding of the interactions between metallic elements (*21*–*23*). Certain complexes spontaneously form M–M bonded units, such as the metal carbonyls (*24*), in response to low coordination number. However, more often than not, the preparation of M–M bonded organometallic compounds requires the strategic stoichiometric reduction of the appropriate mononuclear complexes.

We report here that NHCs are capable of mediating sophisticated organometallic transformations. Depending on the choice of carbene initiator, we observed stoichiometric or catalytic processes, which ultimately produce unexpected organometallic complexes. We propose that the observed reactivity is imparted by the NHCs' ability to induce a key M–M bond-forming reaction.

There is a great need for environmentally friendly and inexpensive alternatives to traditional transition-metal catalysts, and so there has recently been a renaissance in iron-mediated reaction methodology (*25*–*27*). We entered this arena by targeting noncarbonyl, unoxidized iron complexes, bearing monodentate, stable carbene ligands. Such complexes are absent from the literature, and we had hoped that appending NHCs to Fe(0) would afford extremely reactive low-coordinate products. The most direct route to such complexes would be the addition of a carbene to an Fe(0) center, coordinated by labile ligands such as simple arenes or olefins. However, the reported synthetic protocols for such Fe(0) precursors are not practical on a large scale, because they require the vaporization of elemental iron and its co-condensation with the desired ligand (*28*, *29*). A more convenient source of noncarbonyl Fe(0), albeit with a less

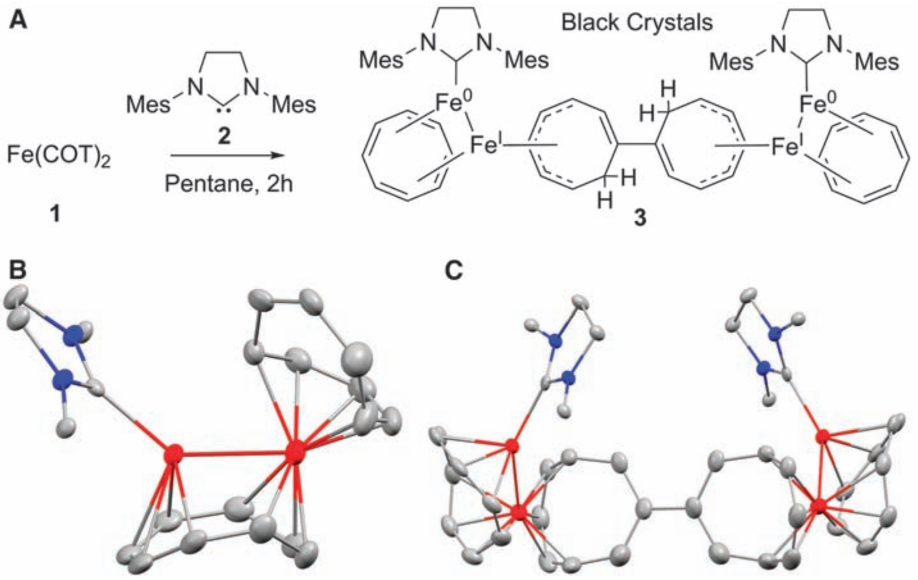

Fig. 1. (**A**) NHC **2** induces the transformation of Fe(COT)$_2$ into the tetrametallic species **3**, featuring two Fe–Fe bonded subunits. The solid-state molecular structure (displacement ellipsoids drawn at the 50% probability level) of **3** is shown in expanded view (**B**) of one of the two equivalent di-iron subunits, and in full (**C**). Red, Fe; gray, C; blue, N. Protons and Mes groups are omitted for clarity.

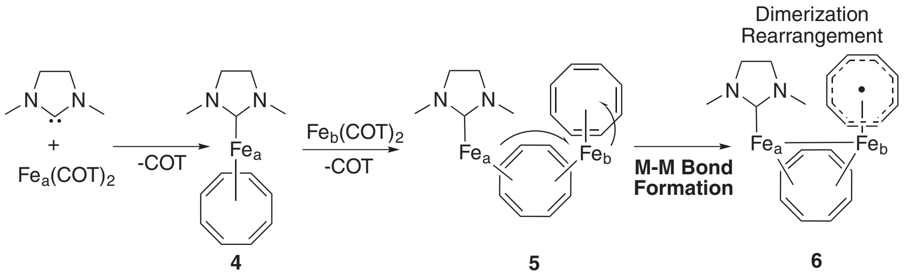

Fig. 2. Proposed pathway for the stoichiometric formation of **3**, with a key NHC-induced M–M bond-forming step.

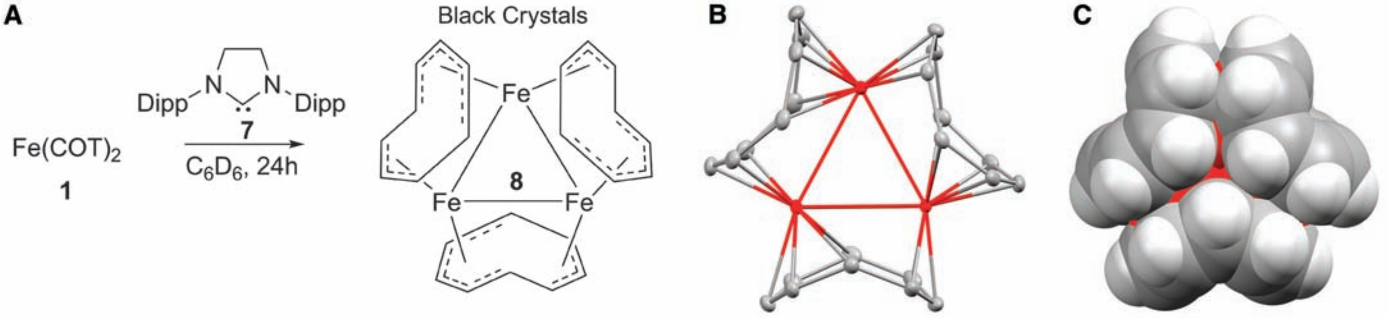

Fig. 3. (**A**) NHC **7** catalyzes the formation of the tri-iron cluster Fe$_3$(COT)$_3$ **8**. The solid-state molecular structure of star-shaped **8**, rendered as balls and sticks (displacement ellipsoids drawn at the 50% probability level; protons omitted for clarity) (**B**), and in space-filling format (**C**) (red, Fe; gray, C; white, H) are shown.

labile hydrocarbon ligand, is bis(cyclooctatetraene) Fe(0), Fe(COT)$_2$ (Fig. 1A, complex **1**) (*30*). This readily available compound has excellent solubility in hydrocarbon solvents and has been reported to undergo the substitution of COT by certain phosphines (*31*).

We chose for a starting carbene ligand the commercially available N,N-bis(2,4,6-trimethyl)phenyl (Mes)–substituted NHC (Fig. 1A, complex **2**). Thus, an unstirred pentane solution of Fe(COT)$_2$ **1** was treated with one equivalent of the NHC **2** at room temperature (Fig. 1) (*32*). Within minutes, small black crystals (Fig. 1A, complex **3**) began to precipitate from the blood-red solution and continued to form over 2 hours. If the reaction was performed using only half an equivalent of NHC **2**, an identical yield (79%) of **3** was obtained. Subsequent proton nuclear magnetic resonance (^{1}H NMR) analysis of the crystalline precipitate redissolved in [D$_6$]benzene revealed resonances ranging from +43.61 to –7.33 parts per million (ppm), which is suggestive of a paramagnetic species. As revealed through a single-crystal x-ray diffraction study of **3** (Fig. 1, B and C), a complicated series of reactions had occurred, resulting in the formation of a tetrametallic species featuring two equivalent di-iron regions. Based on our interpretation of the crystallographic data, the di-iron subunits feature distinctly coordinated Fe(0) and Fe(I) centers: The Fe(0) center is coordinated by the NHC ligand **2** and one half of a COT ring in an η^4-coordination mode; the Fe(I) center shares the other half of this COT ring through η^4binding and is also supported by a separate pentadienyl moiety in a COT-derived ring that connects the two di-iron subunits through a newly formed C–C bond. The close proximity of the mixed valent Fe(0)–Fe(I) centers (Fe–Fe distance, 2.508 Å) suggests an M–M single bond, which would give an overall 16- and 18-electron count at each metal center, respectively. Such mixed-valent Fe(0)–Fe(I) species are of special interest, because they are reminiscent of the elusive proposed intermediate (*33*) in the Fe-only hydrogenase (*34*) cycle.

How does the NHC induce the cascade of reactions that lead to the formation of **3**? We propose that, because the NHC remains coordinated to one of the iron centers in the di-iron subunit, the initial step is the substitution of a single COT ligand from Fe$_a$(COT)$_2$, to afford the highly reactive intermediate (NHC)Fe$_a$(COT) (Fig. 2, complex **4**). Subsequently, the reaction of **4** with Fe$_b$(COT)$_2$ produces the bimetallic intermediate **5**, where both iron atoms are held in close proximity by the bridging COT ligand. At this point the NHC-coordinated Fe$_a$ attacks its stabilized neighbor Fe$_b$, forming an Fe–Fe single bond. In turn, Fe$_b$ transfers a single electron to its nonbridging COT ligand, to afford a ligand-centered radical **6**, which, after dimerization and rearrangement, produces the product **3**.

To further investigate this unusual organometallic transformation, we attempted to prepare a stable version of the initially formed intermediate (NHC)Fe(COT) **4** by using the steric protection of the much bulkier *N*,*N*-bis(2,6-diisopropyl)phenyl (Dipp)–substituted NHC ligand (Fig. 3, ligand **7**). Thus, a [D$_6$]benzene solution of Fe(COT)$_2$ **1** was treated with one equivalent of the NHC **7** at room temperature (Fig. 3A) (*32*). Over a period of 24 hours, the unstirred blood-red solution became orange, and large black rhomboidal crystals (**8**) formed. The crystalline and pyrophoric precipitate **8**, which is nearly insoluble in common organic solvents at room temperature, could be dissolved sufficiently in [D$_6$]benzene for ^{1}H NMR analysis. In solution, **8** exhibits a single, slightly broad (width = 0.40 ppm) paramagnetically shifted resonance at –3.15 ppm, which suggests the formation of a new species that contains iron and at least one coordinated and fluxional COT ligand. Elemental analysis of **8** indicated a compound with an atomic distribution corresponding to a 1:1 ratio of iron and cyclooctatetraene, Fe(COT).

To ascertain the molecular formula and connectivity of **8**, a single-crystal x-ray diffraction study was undertaken. The crystal structure reveals that three Fe(COT) units have been fused to form the tri-iron cluster Fe$_3$(COT)$_3$ **8** (Fig. 3, B and C). The three iron atoms of **8** form an almost perfect equilateral triangle (angles centered at Fe1 = 59.67°, Fe2 = 60.15°, and Fe3 = 60.18°), with an average Fe–Fe distance of 2.824 Å (Fe1–Fe2 = 2.829 Å, Fe1–Fe3 = 2.815 Å, and Fe2–Fe3 = 2.830 Å). The proximity of the iron atoms of **8** suggests direct M–M single bonds (the range for reported Fe–Fe single bonds is 2.20 to 3.12 Å) (*35*), which would give this molecule the expected closed-shell configuration for 48-electron trinuclear clusters (*24*). Each of the three bridging COT ligands adopts coordination modes approaching η^3 and η^5, crowning the iron triangle to form a six-pointed star. A space-filling model of **8** (Fig. 3C) shows that the iron core is completely enveloped by the COT ligands, forming a kinetically protective hydrocarbon shell. The unusual hapticity of the COT ligands suggests that they have a substantial amount of π-allyl and pentadienyl character, which probably results from partial metal-to-ligand electron transfer. However, absent a detailed experimental and computational study of the electronic structure of **8**, we are hesitant to definitively assign the oxidation state of the iron atoms.

Complex **8** is a hydrocarbon analog of the classic tri-iron cluster Fe$_3$(CO)$_{10}$(μ-CO)$_2$, which was discovered over 100 years ago by Dewar and Jones as the first cyclic organometallic cluster compound (*36*). Moreover, Fe$_3$(COT)$_3$ is the only homoleptic trimetallic cluster among group-8 transition metals to bear all-organic, noncarbonyl ligands. The elusiveness of this coordination environment in zero-valent d^8 metal complexes is largely caused by the difficulty of stabilizing such electron-rich clusters without the aid of the strong π-accepting properties of carbonyl ligands.

The observed formation of Fe$_3$(COT)$_3$ **8** is surprising, because Fe(COT)$_2$ **1** has been reported to be indefinitely stable at room temperature in hydrocarbon solvents (*37*); the reaction must be attributed to the presence of the NHC **7**. To explore the catalytic efficiency, we added 10 mole percent of NHC **7** to a benzene solution of Fe(COT)$_2$ **1**, and over a 24-hour period, Fe$_3$(COT)$_3$ **8** slowly crystallized from the reaction mixture in 67% yield, corresponding to a turnover number (TON) of 6.7. If the reaction is conducted at 45°C over the same time period, the yield increases to 95% (TON = 9.5). From control experiments, which were conducted using identical experimental parameters (minus the NHC **7**), we observed that it is possible to detect small amounts of Fe$_3$(COT)$_3$ under forcing conditions (100°C, C$_6$H$_6$, 24 hours) without a catalyst. However, the resultant precipitate is contaminated by copious metallic iron that hampers the purification of **8**.

How does the NHC catalyze the formation of **8**? We believe that the pathway shares common intermediates with the formation of **3**, but the outcomes of these reactions are different based on steric effects of the NHC initiators. We propose that with the larger NHC **7**, the first several steps of these reactions are the same, namely COT displacement (Fig. 4, complex **4′**), combination with Fe(COT)$_2$ **5′**, and Fe–Fe bond for-

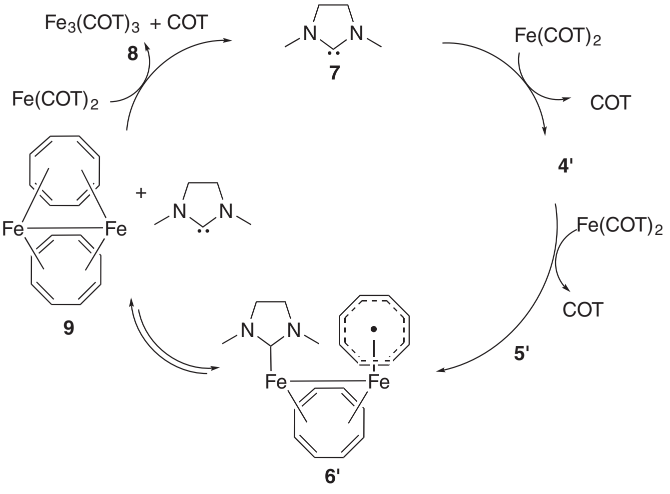

Fig. 4. Proposed catalytic cycle for the formation of **8** mediated by NHC **7** (Dipp groups are omitted for clarity).

mation to afford the ligand-centered radical intermediate **6′**(Fig. 4). In the case of the smaller NHC **2**, because of a lack of kinetic protection as well as strong binding of the carbene ligand, the dimerization process of **6** proceeds and the mixed valent Fe(0)–Fe(I) species is formed stoichiometrically (Fig. 2). However, when the more sterically demanding NHC **7** interacts with the iron center, the dimerization process is blocked, and the unstable species **6′** extrudes the NHC ligand. The ensuing $Fe_2(COT)_2$ species rapidly combines with $Fe(COT)_2$ to form the tri-iron cluster. Of course, it is possible that the NHC may not dissociate until the third Fe(COT) fragment is added to **6′**. There is ample precedent in the literature for NHC lability, particularly in zero-valent, late transition-metal complexes (*38*). Moreover, steric hindrance at the metal center reportedly facilitates this process (*39*).

Once thought of only as laboratory curiosities, stable carbenes are now widely recognized as indispensable tools for organic synthesis. The NHC-mediated reactions we explored provide a foundation on which to develop future organometallic transformations catalyzed by NHCs, as well as other small organic species.

References and Notes

1. R. A. Moss, M. S. Platz, M. Jones Jr., Eds., *Reactive Intermediate Chemistry* (Wiley, New York, 2004).
2. A. Igau, H. Grutzmacher, A. Baceiredo, G. Bertrand, *J. Am. Chem. Soc.* **110**, 6463 (1988).
3. A. J. Arduengo, R. L. Harlow, M. Kline, *J. Am. Chem. Soc.* **113**, 361 (1991).
4. F. E. Hahn, M. C. Jahnke, *Angew. Chem. Int. Ed.* **47**, 3122 (2008).
5. R. H. Crabtree, *Coord. Chem. Rev.* **251**, 595 (2007).
6. J. Vignolle, X. Catton, D. Bourissou, *Chem. Rev.* **109**, 3333 (2009).
7. O. Schuster, L. Yang, H. G. Raubenheimer, M. Albrecht, *Chem. Rev.* **109**, 3445 (2009).
8. M. Alcarazo, C. W. Lehmann, A. Anoop, W. Thiel, A. Fürstner, *Nat. Chem.* **1**, 295 (2009).
9. O. Kaufhold, F. E. Hahn, *Angew. Chem. Int. Ed.* **47**, 4057 (2008).
10. V. Lavallo, Y. Canac, B. Donnadieu, W. W. Schoeller, G. Bertrand, *Angew. Chem. Int. Ed.* **45**, 3488 (2006).
11. J. D. Masuda, W. W. Schoeller, B. Donnadieu, G. Bertrand, *Angew. Chem. Int. Ed.* **46**, 7052 (2007).
12. G. D. Frey, V. Lavallo, B. Donnadieu, W. W. Schoeller, G. Bertrand, *Science* **316**, 439 (2007).
13. Y. Z. Wang *et al.*, *Science* **321**, 1069 (2008).
14. D. Enders, A. A. Narine, *J. Org. Chem.* **73**, 7857 (2008).
15. R. H. Grubbs, *Angew. Chem. Int. Ed.* **45**, 3760 (2006).
16. C. Samojłowicz, M. Bieniek, K. Grela, *Chem. Rev.* **109**, 3708 (2009).
17. R. Breslow, E. Mcnelis, *J. Am. Chem. Soc.* **81**, 3080 (1959).
18. D. Enders *et al.*, *Angew. Chem. Int. Ed. Engl.* **34**, 1021 (1995).
19. N. Marion, S. Diez-Gonzalez, S. P. Nolan, *Angew. Chem. Int. Ed.* **46**, 2988 (2007).
20. D. A. Culkin *et al.*, *Angew. Chem. Int. Ed.* **46**, 2627 (2007).
21. I. Resa, E. Carmona, E. Gutierrez-Puebla, A. Monge, *Science* **305**, 1136 (2004).
22. T. Nguyen *et al.*, *Science* **310**, 844 (2005).
23. S. P. Green, C. Jones, A. Stasch, *Science* **318**, 1754 (2007).
24. P. J. Dyson, J. S. McIndoe, *Transition Metal Carbonyl Cluster Chemistry* (Gordon & Breach, Amsterdam, 2000).
25. C. Bolm, J. Legros, J. Le Paih, L. Zani, *Chem. Rev.* **104**, 6217 (2004).
26. B. D. Sherry, A. Fürstner, *Acc. Chem. Res.* **41**, 1500 (2008).
27. A. Fürstner, *Angew. Chem. Int. Ed.* **48**, 1364 (2009).
28. R. Mackenzi, P. L. Timms, *J. Chem. Soc. Chem. Commun.* 650 (1974).
29. P. Le Floch *et al.*, *Eur. J. Inorg. Chem.* **1998** (1998).
30. D. H. Gerlach, R. A. Schunn, *Inorg. Syn.* **15**, 2 (1974).
31. H. Felkin, P. W. Lednor, J. M. Normant, R. A. J. Smith, *J. Organomet. Chem.* **157**, C64 (1978).
32. Materials and methods are detailed in supporting material available on *Science* Online.
33. M. Y. Darensbourg, E. J. Lyon, X. Zhao, I. P. Georgakaki, *Proc. Natl. Acad. Sci. U.S.A.* **100**, 3683 (2003).
34. J. W. Peters, W. N. Lanzilotta, B. J. Lemon, L. C. Seefeldt, *Science* **282**, 1853 (1998).
35. C. R. Hess, T. Weyhermuller, E. Bill, K. Wieghardt, *Angew. Chem. Int. Ed.* **48**, 3703 (2009).
36. R. Desiderato, G. R. Dobson, *J. Chem. Educ.* **59**, 752 (1982).
37. A. Carbonaro, A. Greco, G. Dallasta, *J. Organomet. Chem.* **20**, 177 (1969).
38. N. D. Clement, K. J. Cavell, L. L. Ooi, *Organometallics* **25**, 4155 (2006).
39. R. Dorta *et al.*, *J. Am. Chem. Soc.* **127**, 2485 (2005).
40. We gratefully acknowledge financial support from NIH for grant 5RO1 GM31332 and a National Research Service Award Postdoctoral Fellowship (to V.L.). We thank L. M. Henling and M. W. Day (California Institute of Technology) for x-ray crystallographic analysis. The Bruker KAPPA APEX II x-ray diffractometer was purchased via an NSF Chemistry Research Instrumentation and Facilities: Multi-User award to the California Institute of Technology, CHE-0639094. Crystallographic data for complexes **3** and **8** are available free of charge from the Cambridge Crystallographic Data Center under reference numbers CCDC-724011 and CCDC-728138, respectively.

Supporting Online Material
www.sciencemag.org/cgi/content/full/326/5952/559/DC1
Materials and Methods
References

10 July 2009; accepted 13 August 2009
10.1126/science.1178919

Detection of Adsorbed Water and Hydroxyl on the Moon

Roger N. Clark

Data from the Visual and Infrared Mapping Spectrometer (VIMS) on Cassini during its flyby of the Moon in 1999 show a broad absorption at 3 micrometers due to adsorbed water and near 2.8 micrometers attributed to hydroxyl in the sunlit surface on the Moon. The amounts of water indicated in the spectra depend on the type of mixing and the grain sizes in the rocks and soils but could be 10 to 1000 parts per million and locally higher. Water in the polar regions may be water that has migrated to the colder environments there. Trace hydroxyl is observed in the anorthositic highlands at lower latitudes.

The quest to find water on the Moon has been underway since the prediction of ice in the permanently shadowed craters in the polar regions (*1*, *2*). Water is a vital resource needed by a human colony and played a fundamental role in planetary evolution (*3*). Spectroscopy is a tool that can be used to detect water and hydroxyl in the optical surface (the top few mm) using OH and H_2O absorptions near 1.5, 2, and 3 µm.

It is thought that the Moon formed by a collision between Earth and a Mars-sized body (*4*) about 4.4×10^9 years ago. The impact and the accretion of the debris heated the early Moon, creating an extensive lunar magma ocean (*5*, *6*). These events are thought to have resulted in the loss of almost all volatiles in the Moon, and indeed evidence from Apollo and Luna samples indicate that lunar materials are deficient in volatiles compared with Earth (*3*). However, 20 to 45 parts per million (ppm) water occurs in some Apollo lunar glasses (*7*).

In addition, neutron spectrometer data from Lunar Prospector (LP) (*8*–*10*) showed that hydrogen is present in the lunar polar regions. I used data from the Visual and Infrared Mapping Spectrometer (VIMS) (*11*) on Cassini, which flew by the Moon on 19 August 1999, to map the distribution of water (Fig. 1). VIMS obtained 11 full and 2 partial image cubes with a spatial resolution of about 175 km per pixel and spectral coverage over the 0.35 to 5 µm with some gaps due to sensor saturation [supporting online material (SOM) text and fig. S1].

Where the moon is warmed by solar radiation, thermal emission contributes to the observed signal, $(I + T)/F$, where I is measured radiance plus thermal emission T and πF equals solar radiance. The thermal emission component and emissivity effects can mask weak water absorptions, but not strong ones, nor sharper absorptions due to hydroxyl. Thermal emission was computed and removed from lunar spectra (Fig. 2A) by using a thermal model (*12*, *13*) (SOM text and figs. S2 and S3), which included estimating the emissivity from reflectance by using Kirchoff's law. Thermal-removed lunar spectra show water and hydroxyl absorptions in many but not all locations on the lunar disk (Figs. 1, E and F, and 2, A and B). The linear, positive-sloping spectral shape (Fig. 2A) is characteristic of the spectral signature of nanophase iron (*14*).

The lunar absorptions near 3 µm are characteristic of an O-H stretch fundamental in the H_2O molecule commonly seen in spectra of materials with adsorbed water or hydroxyl-bearing materials (Fig. 2, C and D) (*15*). The VIMS broad 3-µm absorption was strongest in the south lunar

---

U.S. Geological Survey, Mail Stop 964, Box 25046 Federal Center, Denver, CO 80227, USA. E-mail: rclark@usgs.gov